

A boron-containing molecule as an efficient electron-transporting material with low-power consumption

Katsuyuki Shizu,¹ Tohru Sato,^{1,2,a)} Kazuyoshi Tanaka,¹ and Hironori Kaji³

¹Department of Molecular Engineering, Graduate School of Engineering, Kyoto University, Nishikyo-ku, Kyoto 615-8510, Japan

²Fukui Institute for Fundamental Chemistry, Kyoto University, Takano-Nishihiraki-cho 34-4, Sakyo-ku, Kyoto 606-8103, Japan

³Institute for Chemical Research, Kyoto University, Gokasho, Uji, Kyoto 611-0011, Japan

(Received 9 August 2010; accepted 17 September 2010; published online 8 October 2010)

We theoretically propose a boron-containing molecule, hexaboracyclophane (HBCP), as an electron-transporting (ET) material with low-power loss. We calculate the vibronic coupling of HBCP, comparing them with those of other ET materials, tris-(8-hydroxyquinoline) aluminum(III) (Alq₃) and tris[3-(3-pyridyl)mesityl]borane (3TPYMB). Using the nonequilibrium Green's function method to evaluate their single molecular ET properties, we show that HBCP exhibits more efficient and lower-power consumption than Alq₃ and 3TPYMB. HBCP has suitable occupied molecular orbital and lowest unoccupied molecular orbital energy levels as an electron-transport layer when Alq₃ is employed as an emitter. © 2010 American Institute of Physics.

[doi:10.1063/1.3499310]

Organic light-emitting diodes (OLEDs) have been of great interest because of their potential application for large-area full-color flat-panel displays. To enhance device efficiency it is necessary to develop electron-transporting materials with high-electron mobility and improve charge balance in OLEDs.¹ Alq₃ is one of the most widely used electron-transporting material in OLEDs and also used as a green emitter.^{2,3} On the other hand, various boron-containing π -conjugated systems have electron-transporting property,⁴⁻⁹ suggesting that boron plays a key role in electron-transporting process. Recently, Tanaka *et al.*⁹ have reported that tris[3-(3-pyridyl)mesityl]borane (3TPYMB) exhibits electron mobility about ten times higher than that of Alq₃ and has hole-blocking property.

One of the factors that controls the electron mobility is intramolecular vibronic coupling (electron-molecular vibration interaction). Inelastic scattering due to vibronic coupling not only inhibits electron transport and reduces electron mobility but also causes Joule heat or power loss. Crystallization or melting of organic materials due to Joule heat is an origin of the instability of OLEDs.¹⁰ Hence, molecules with weak vibronic coupling are favorable for electron-transporting material. In this letter, we theoretically propose a boron-containing electron-transporting material, hexaboracyclophane (HBCP) (Fig. 1) and compare its vibronic coupling, electron-transporting property, and hole-blocking character with those of *mer*-Alq₃ and 3TPYMB.

The strength of vibronic coupling of the i^{th} mode is controlled by the vibronic coupling constant (VCC) V_i . V_i can be expressed as $V_i = \int \Delta\rho \times v_i d\tau$, where $\Delta\rho$ is an electron-density difference between neutral and anion states and v_i is one-electron part of the derivative of the nuclear-electronic potential with respect to the i^{th} normal coordinate.¹¹ Note that only totally symmetric modes couple to the electronic states and have nonzero V_i values. Geometry optimization and vi-

brational analysis for neutral *mer*-Alq₃, 3TPYMB, and HBCP were done at the B3LYP/3-21G level of theory. We assumed C_1 , C_3 , and D_6 symmetries for *mer*-Alq₃, 3TPYMB, and HBCP, respectively. The electronic structures of anionic states for these molecules were calculated at the UB3LYP/3-21G level of theory using the optimized geometries of the neutral states. A scaling factor of 0.963 (Ref. 12) was used for B3LYP/3-21G theoretical frequencies. All the *ab initio* calculations were done using GAUSSIAN 03 software.¹³ We calculated current through a single *mer*-Alq₃/3TPYMB/HBCP molecule employing the nonequilibrium Green's function (NEGF) method taking into account inelastic scattering due to vibronic coupling.¹⁴

Figures 2(a)–2(c) show VCCs of *mer*-Alq₃, 3TPYMB, and HBCP. *mer*-Alq₃ has the largest V_i and exhibits the strongest vibronic coupling among them. Since *mer*-Alq₃ belongs to C_1 symmetry, all the vibrational modes (150 modes) have nonzero V_i . Low-symmetry molecular structure and not small V_i values lead to stronger vibronic coupling of *mer*-Alq₃ than those of 3TPYMB and HBCP. However, the

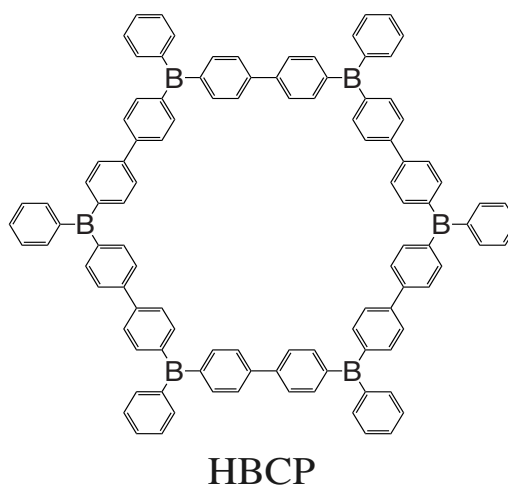
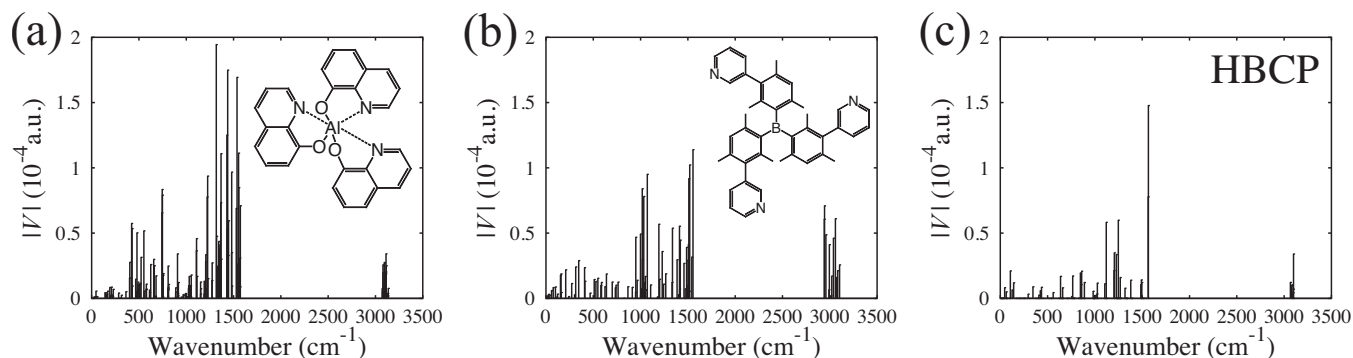


FIG. 1. Chemical structure of HBCP.

^{a)}Author to whom correspondence should be addressed. Electronic mail: tsato@scl.kyoto-u.ac.jp.

FIG. 2. VCCs of (a) *mer*-Alq₃, (b) 3TPYMB, and (c) HBCP.

largest V_i of *mer*-Alq₃ is at most 2.0×10^{-4} a.u., which is small compared with biphenyl, fluorene, and carbazole,¹⁵ indicating that the vibronic coupling in *mer*-Alq₃ is weak as a π -conjugated system.

The largest V_i of 3TPYMB is about 1.2×10^{-4} a.u. [Fig. 2(b)]. This value is quite small and comparable to the vibronic coupling in the cationic state of *N,N'*-bis(3-methylphenyl)-*N,N'*-diphenyl-[1,1'-biphenyl]-4,4'-diamine,¹¹ which is a widely used hole-transporting material in OLEDs. The number of vibrational modes of 3TPYMB (258 modes) is larger than that of *mer*-Alq₃. However, the number of totally symmetric modes of 3TPYMB (86 modes) is smaller than that of *mer*-Alq₃ because of the existence of the C_3 axis. The smaller V_i values and number of totally symmetric modes are responsible for the weaker vibronic coupling in 3TPYMB than in *mer*-Alq₃.

Figure 2(c) shows V_i of HBCP. Although HBCP has the largest molecular size and the number of vibrational modes (570 modes) among the three molecules, it has the smallest number of totally symmetric modes (46 modes) because of its high symmetry. Thus, high symmetry reduces the number of totally symmetric modes, and consequently, weakens the vibronic coupling as a whole. Furthermore, the largest V_i of HBCP is relatively small (1.6×10^{-4} a.u.) and the other V_i values are of the order of 1×10^{-5} a.u. and quite small. The high symmetry and small V_i values of HBCP make it a promising candidate for an electron-transporting material.

Figure 3 shows highest occupied molecular orbital (HOMO) and lowest unoccupied molecular orbital (LUMO)

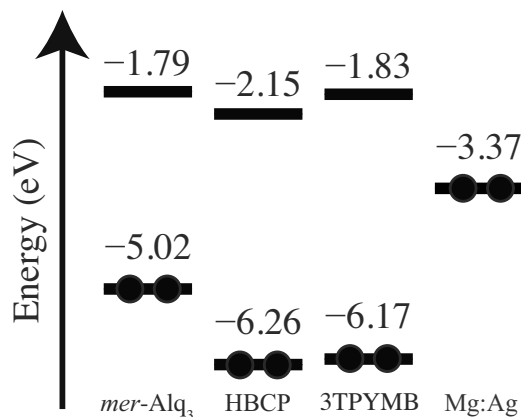


FIG. 3. HOMO/LUMO energy-level diagrams for *mer*-Alq₃, 3TPYMB, and HBCP calculated at the B3LYP/3-21G level of theory. The experimental work function with opposite sign of an Mg:Ag alloy (see Ref. 16) is shown as the Fermi energy of Mg:Ag electrode surface.

energy levels of *mer*-Alq₃, 3TPYMB, and HBCP calculated at the B3LYP/3-21G level of theory and Fermi energy of the Mg:Ag electrode, which is a typical cathode for OLEDs. The Fermi energy shown here is the experimental work function of the Mg:Ag alloy with the opposite sign.¹⁶ The HOMO/LUMO energy level of HBCP is lower than that of 3TPYMB and hence, HBCP is expected to be a better electron-injecting and hole-blocking material than 3TPYMB when *mer*-Alq₃ is used as an emitting layer.

To investigate a suppression effect of vibronic coupling on electric current we calculated current-voltage (I - V_b) characteristics for a single *mer*-Alq₃/3TPYMB/HBCP molecule using the NEGF method.¹⁴ Here, we considered neighboring molecules in a solid as a part of electrodes and set their Fermi levels to be the HOMO levels shown in Fig. 3. We used the electronic coupling $\tau=0.5$ eV and temperature $T=298$ K. In the NEGF method, the I - V_b characteristics are influenced by τ and V_i . Since we focus on a suppression effect due to the vibronic coupling on I - V_b characteristics, τ was set to be the same value for the three molecules.

Figure 4(a) shows the I - V_b characteristics for *mer*-Alq₃ (dotted line), 3TPYMB (dashed line), and HBCP (solid line). Significantly, HBCP exhibits the largest I , suggesting that for HBCP, the suppression effect due to vibronic coupling is weak compared with *mer*-Alq₃ and 3TPYMB, and HBCP can be a superior electron-transporting material than *mer*-Alq₃ and 3TPYMB. The large I originates from the high-symmetry and small V_i values of HBCP. Since the vibronic coupling in 3TPYMB is weaker than in *mer*-Alq₃, 3TPYMB exhibits larger I than *mer*-Alq₃. This result is consistent with the experimental observation that 3TPYMB exhibits higher electron mobility than *mer*-Alq₃.⁹ The weak vibronic coupling is an origin of the high electron mobility of 3TPYMB. Inelastic scattering due to vibronic coupling causes power loss, in other words, heat generation. Figure 4(b) shows power loss in a single *mer*-Alq₃/3TPYMB/HBCP molecule. The power loss decreases in the following order: *mer*-Alq₃ > 3TPYMB > HBCP, suggesting that molecules with weak vibronic coupling exhibit low power consumption.

In conclusion, we designed the boron-containing molecule with high-symmetry, HBCP. The theoretically designed HBCP exhibits weaker vibronic coupling and higher electron-transporting property than *mer*-Alq₃ and 3TPYMB. Furthermore, since the HOMO/LUMO energy level of HBCP is lower than that of 3TPYMB, HBCP can be a superior electron-injecting and hole-blocking material than 3TPYMB when *mer*-Alq₃ is used as an emitting layer. In

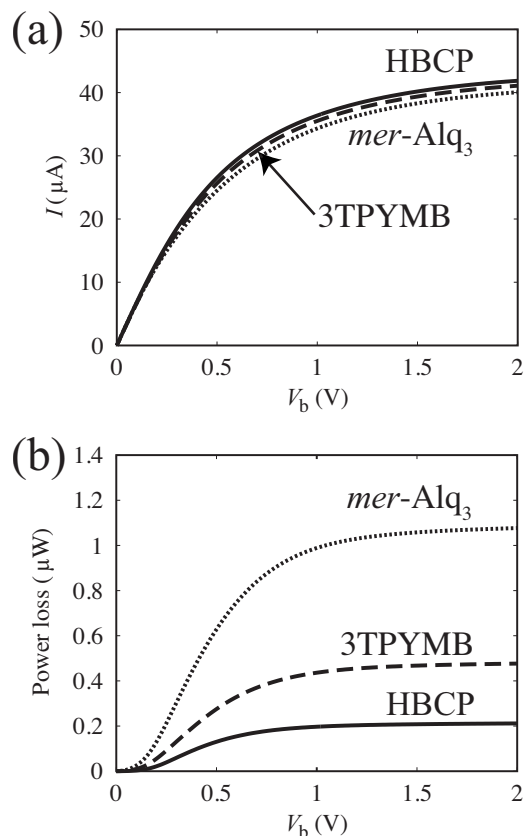


FIG. 4. (a) Current-voltage characteristics and (b) power loss for *mer*-Alq₃ (dotted lines), 3TPYMB (dashed lines), and HBCP (solid lines).

actual synthesis, it is necessary to protect the boron atoms, for instance, by introducing the methyl group at the ortho positions of the phenyl and phenylene groups. Such a chemical modification would change torsion angles between phenyl rings but would not impair the electron-transporting and hole-blocking properties of HBCP so much. We calculated reorganization energies and HOMO/LUMO energy levels at the B3LYP/3-21G and UB3LYP/3-21G levels of theory for one-third-sized fragments of unsubstituted and methyl-substituted HBCP. The difference between the reorganization energies and HOMO/LUMO energy levels for the two molecules are 24 meV and 0.09/0.42 eV, respectively, suggesting that the electron-transporting and hole-blocking properties of HBCP are not influenced significantly by the methyl substitution. Usually, amorphous materials have been used in OLEDs. HBCP might be highly crystalline in nature because of its high symmetry. Amorphous HBCP-based materials would be obtained, for example, by introducing bulky substituents into HBCP.

The authors thank Professor Yoshihiro Matano (Kyoto University) for helpful discussion. Numerical calculations were performed partly in the Supercomputer Laboratory of Kyoto University and Research Center for Computational Science, Okazaki, Japan. This work was supported in part by the Japan Society for the Promotion of Science (JSPS) through its Funding Program for Scientific Research (C) (Grant No. 20550163), Priority Areas “Molecular theory for real systems” (Grant No. 20038028), for World-Leading Innovative R&D on Science and Technology (FIRST Program), and for the Global COE Program “International Center for Integrated Research and Advanced Education in Materials Science” (Grant No. B-09) of the Ministry of Education, Culture, Sports, Science, and Technology (MEXT) of Japan.

¹N. Chopra, J. Lee, Y. Zheng, S.-H. Eom, J. Xue, and F. So, *Appl. Mater. Interfaces* **1**, 1169 (2009).

²C. W. Tang and S. A. VanSlyke, *Appl. Phys. Lett.* **51**, 913 (1987).

³C. W. Tang, S. A. VanSlyke, and C. H. Chen, *J. Appl. Phys.* **65**, 3610 (1989).

⁴T. Noda and Y. Shirota, *J. Am. Chem. Soc.* **120**, 9714 (1998).

⁵S. Yamaguchi, S. Akiyama, and K. Tamao, *J. Am. Chem. Soc.* **122**, 6335 (2000).

⁶Q. Wu, M. Esteghamatian, N.-X. Hu, Z. Popovic, G. Enright, Y. Tao, M. D'Iorio, and S. Wang, *Chem. Mater.* **12**, 79 (2000).

⁷M. Kinoshita and Y. Shirota, *Chem. Lett.* **30**, 614 (2001).

⁸M. Kinoshita, H. Kita, and Y. Shirota, *Adv. Funct. Mater.* **12**, 780 (2002).

⁹D. Tanaka, T. Takeda, T. Chiba, S. Watanabe, and J. Kido, *Chem. Lett.* **36**, 262 (2007).

¹⁰Y. Shirota, Y. Kuwabara, D. Okuda, R. Okuda, H. Ogawa, H. Inada, T. Wakimoto, H. Nakada, Y. Yonemoto, S. Kawami, and K. Imai, *J. Lumin.* **72-74**, 985 (1997).

¹¹T. Sato, K. Shizu, T. Kuga, K. Tanaka, and H. Kaji, *Chem. Phys. Lett.* **458**, 152 (2008).

¹²G. Rauhut and P. Pulay, *J. Phys. Chem.* **99**, 3093 (1995).

¹³M. J. Frisch, G. W. Trucks, H. B. Schlegel, G. E. Scuseria, M. A. Robb, J. R. Cheeseman, J. A. Montgomery, Jr., T. Vreven, K. N. Kudin, J. C. Burant, J. M. Millam, S. S. Iyengar, J. Tomasi, V. Barone, B. Mennucci, M. Cossi, G. Scalmani, N. Rega, G. A. Petersson, H. Nakatsuji, M. Hada, M. Ehara, K. Toyota, R. Fukuda, J. Hasegawa, M. Ishida, T. Nakajima, Y. Honda, O. Kitao, H. Nakai, M. Klene, X. Li, J. E. Knox, H. P. Hratchian, J. B. Cross, V. Bakken, C. Adamo, J. Jaramillo, R. Gomperts, R. E. Stratmann, O. Yazyev, A. J. Austin, R. Cammi, C. Pomelli, J. W. Ochterski, P. Y. Ayala, K. Morokuma, G. A. Voth, P. Salvador, J. J. Dannenberg, V. G. Zakrzewski, S. Dapprich, A. D. Daniels, M. C. Strain, O. Farkas, D. K. Malick, A. D. Rabuck, K. Raghavachari, J. B. Foresman, J. V. Ortiz, Q. Cui, A. G. Baboul, S. Clifford, J. Cioslowski, B. B. Stefanov, G. Liu, A. Liashenko, P. Piskorz, I. Komaromi, R. L. Martin, D. J. Fox, T. Keith, M. A. Al-Laham, C. Y. Peng, A. Nanayakkara, M. Challacombe, P. M. W. Gill, B. Johnson, W. Chen, M. W. Wong, C. Gonzalez, and J. A. Pople, *GAUSSIAN 03, Revision D.02* (Gaussian, Wallingford, CT, 2004).

¹⁴S. Datta, *Quantum Transport: Atom to Transistor* (Cambridge University Press, Cambridge, 2005).

¹⁵K. Shizu, T. Sato, K. Tanaka, and H. Kaji, *Org. Electron.* **11**, 1277 (2010).

¹⁶P. A. Lane, G. P. Kushto, and Z. H. Kafafi, *Appl. Phys. Lett.* **90**, 023511 (2007).